Passive Mode Locking of Lasers by Crossed-Polarization Gain Modulation

Julien Javaloyes, Josep Mulet, and Salvador Balle
Institut Mediterrani d'Estudis Avançats (IMEDEA), CSIC-UIB, Campus Universitat de les Illes Balears, E-07122 Palma de Mallorca, Spain
(Received 9 May 2006; published 16 October 2006)

We report on a novel approach for inducing passive mode locking of lasers without using any saturable absorber but exploiting the polarization degree of freedom of light. In our scheme, passive mode locking is achieved by crossed-polarization gain modulation caused by the reinjection of a polarization-rotated replica of the laser output after a time delay. The reinjection time delay defines resonance tongues that correspond to mode-locking operation. Numerical continuation reveals that the cw solution is destabilized through a Hopf bifurcation that defines the onset of multimode operation which evolves sharply into a mode-locked solution. Our approach can be applied to a large variety of laser systems. For vertical-cavity surface-emitting lasers, we demonstrate stable mode-locked pulses at repetition rates in the GHz range and pulse widths of few tens of picoseconds.

DOI: 10.1103/PhysRevLett.97.163902 PACS numbers: 42.60.Fc, 42.55.Px, 42.65.Sf

Mode locking (ML) of lasers has been a subject of intense research because of the complex nonlinear dynamics involving the self-organization of many laser modes [1]. Added relevance to ML is the large number of present applications in medicine, metrology, and telecommunications [2]. ML has led to the shortest and most intense optical pulses ever generated.

A multimode laser can be forced to operate in a mode-locked state either passively or actively. Active ML is achieved by modulating one control parameter of the laser at a frequency resonant with the separation between longitudinal modes. A drawback of active ML is the requirement of a precise external modulation which can be unreachable at ultrafast speeds. An alternative is provided by the all-optical active ML techniques, e.g., induced by externally injecting a train of optical pulses at a subharmonic of the repetition frequency [3]. On the other hand, passive ML (PML) does not require any external modulation and it is the preferred approach for generating optical pulses at multi-GHz repetition rates [2]. PML is commonly achieved by combining two elements, a laser amplifier which provides gain and a saturable absorber acting as a pulse shortening element. A window for amplification is opened around the pulse due to the faster recovery time of the absorption. The technological difficulties of making faster absorbers stimulated the search for ''artificial'' saturable absorbers which are characterized by ultrafast intensity-dependent losses, e.g., additive-pulse ML, nonlinear polarization rotation (NLPR), and Kerr lens mode locking (KLM) [4]. Among these methods, NLPR takes advantage of the lightwave polarization degree of freedom and it has recently been demonstrated in ML semiconductor lasers [5].

In this Letter, we report on a novel approach for inducing passive mode locking in laser systems without using any saturable absorber but directly exploiting the polarization degree of freedom of light. In our approach, the laser amplifier plays a twofold role, i.e., to provide amplification and the nonlinearities for pulse shortening. PML is achieved by crossed-polarization gain modulation (XPGM) [6,7] in the laser amplifier caused by the reinjection of a polarization-rotated replica of the laser output after a time delay. The proposed mechanism for PML is generic of lasers and reminiscent of the situations of delayed coupling between two lasers explored in [8]. In this Letter, it will be analyzed in detail for a vertical-external-cavity surface-emitting laser (VECSEL). Although VECSELs have been passively mode locked with saturable absorbers [9], polarization has not yet been exploited for these purposes. We shall demonstrate that our scheme can be used to generate robust PML at repetition rates in the GHz range and pulse widths of few tens of picoseconds.

A particular realization of our proposal is schematically shown in Fig. 1. We consider a vertical-cavity surface-emitting laser (VCSEL) supporting only the fundamental transverse mode in any of the two possible polarization orientations. The VCSEL is coupled to an external cavity defined by a partially reflective mirror r_3. A polarizing beam splitter (PBS) is inserted in the external cavity, thus one of the linear polarization (LP) components of the light (x) is fed back into the VCSEL after a round-trip time τ_1.

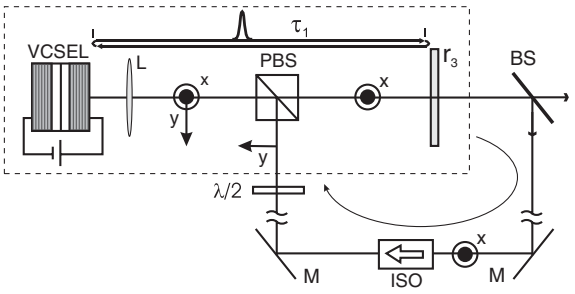

FIG. 1. Mode-locked laser setup comprising an external-cavity VCSEL (dashed box) and a reinjection arm. Symbols: polarizing beam splitter (PBS), optical isolator (ISO), and half-wavelength plate ($\lambda/2$).

The orthogonal LP component (y) is expelled from the external cavity. Hence, the dashed box in the figure defines a multi-longitudinal-mode VECSEL, whose output through r_3 is always x_{LP}. A fraction of this output is reinjected into the VCSEL through the PBS after a time delay τ_2. An optical isolator (ISO) is inserted in order to ensure unidirectional operation of the reinjection arm, and a $\lambda/2$ plate converts the polarization to y_{LP}. In this way, the VCSEL is subject to injection in the polarization direction that is unfavored by the feedback from the external mirror. In the active medium, both polarizations interact via XPGM.

We describe the system shown in Fig. 1 using the so-called spin-flip model [10], modified in order to take into account the effects of optical feedback and reinjection as done in Ref. [11]. Extensive numerical simulations demonstrate that the onset of mode locking is robust against the inclusion of the linear anisotropies and spin-flip processes for typical values of these parameters. For the sake of simplicity, in this Letter we shall describe VCSEL dynamics assuming vanishingly small anisotropies and fast spin-flip relaxation rates. The resulting equations describing the temporal evolution of the LP electric fields $E_{x,y}$ at the active medium and the population inversion N read

$$\dot{E}_x = (1 + i\alpha)NE_x + \eta e^{-i\Omega}E_x(t - \tau_1), \tag{1}$$

$$\dot{E}_y = (1 + i\alpha)NE_y + \beta E_x(t - \tau_2), \tag{2}$$

$$T\dot{N} = P - N - (1 + 2N)(|E_x|^2 + |E_y|^2). \tag{3}$$

In Eq. (1) we have assumed weak feedback conditions. The meaning of the different dimensionless parameters in Eqs. (1)–(3) is the following: η and Ω are the feedback strength and phase, β the reinjection strength, τ_1 the external-cavity round-trip time, τ_2 the reinjection delay time, and T the population lifetime. P is the scaled pump excess and α the amplitude-phase coupling factor. The injection strength β is taken real and positive by a global phase redefinition. The time is scaled to the photon lifetime of the VCSEL which amounts to $1/\kappa = 1$ ps. The remaining parameter values are: $\Omega = 0$, $\tau_1 = 1000$, $T = 500$, and $\alpha = 3$. We consider η, β, P, and τ_2 as control parameters.

The dynamics of the external-cavity laser without reinjection has been thoroughly studied in the literature for different feedback regimes [12]. Although regular pulse packages [13] and more complex dynamics have been reported, to our knowledge, no regimes of stable PML operation have ever been found.

The addition of reinjection substantially modifies the scenario. For appropriate reinjection conditions, the laser output consists of a periodic train of short and intense pulses whose period matches the round-trip time τ_1 in the external cavity. The most favorable situation for mode locking is achieved for $\beta \gtrsim \eta$. This regime is stable against noise and appears in wide parameter ranges, e.g., for pumping ranging from below to above the solitary laser threshold. Figure 2(a) shows a typical pulse train obtained by numerical integration of Eqs. (1)–(3). Both intensities $I_{x,y}(t) = |E_{x,y}(t)|^2$ in the active medium exhibit similar time traces, the latter being a scaled and delayed replica of the former. The temporal shift of the two traces is determined by $\Delta\tau = \tau_2 - \tau_1$. The temporal pulse width in this example is $\sim$30 ps, which is in the state of the art of electrically-driven VECSELs mode locked with saturable absorbers [9,14]. The optical spectrum of the output shows that pulsed operation appears in connection with multimode emission [Fig. 2(b)]. The different peaks in the frequency comb are separated by $1/\tau_1$ as a characteristic of mode locking. The spectral width of the pulses is of the order of 20 GHz, which roughly corresponds to the available optical bandwidth of the system.

The evolution of the population inversion in Fig. 2(c) shows that the arrival of a x_{LP} pulse induces a fast depletion of the population which roughly lasts a pulse width. This fast stage is followed by a slow recovery which is interrupted by the arrival of a y_{LP} pulse after a delay $\Delta\tau(\mathrm{mod}\tau_1)$. This pulse causes another fast depletion of the population down to its lowest value. From there on, the population exhibits a second slow recovery until the next x_{LP} pulse arrives. The whole process repeats every period τ_1. Figure 3 shows the resulting trajectory in a phase space projection with variables $(I_x(t), I_y(t), N(t))$. The label (a) indicates the instant at which the population reaches the maximum value, and (b) the depletion caused by the x_{LP} pulse. If no other optical pulse would arrive after this point, the system might undergo relaxation oscillations eventually yielding a steady state. The arrival of the orthogonally polarized pulse with correct lag $\Delta\tau$ around the vicinity of the point (b) effectively enhances the population pulsa-

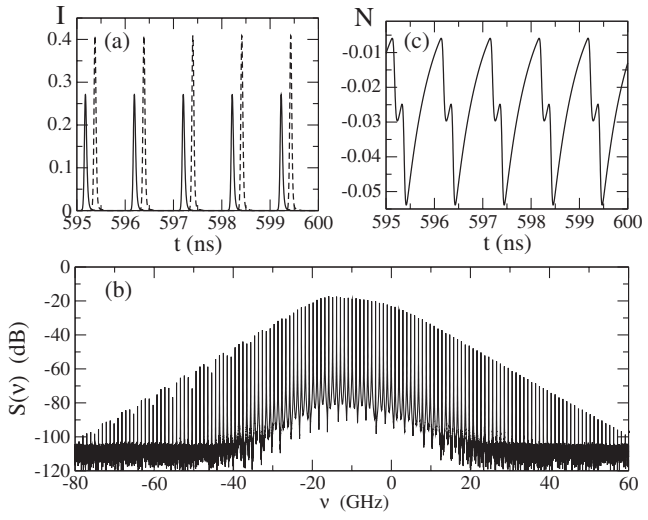

FIG. 2. (a) Time traces of the LP components, x_{LP} (y_{LP}) in solid (dashed) line. (b) Optical spectrum of the x_{LP} component. (c) Evolution of the population inversion. Parameters: $\eta = 0.02$, $\beta = 0.06$, $P = 0.01$, and $\tau_2 = 1.2\tau_1$.

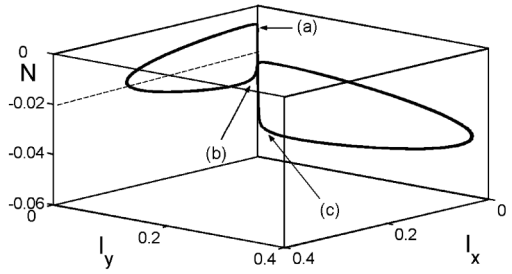

FIG. 3. Phase space portrait of the system trajectory.

tions. As shown in the figure, the system is forced to switch from the plane N-I_x to the plane N-I_y, and in this process the population is further depleted down to point (c).

In order to disclose some qualitative features of the system, Fig. 4(a) shows the computed bifurcation diagram for the extrema of the x_{LP} intensity I_x upon increasing the reinjection delay time τ_2 at a fixed reinjection strength. The bifurcation diagram for I_y is similar to that shown in the figure. At a fixed τ_2, a single point in the diagram stands for cw operation, two points for stable pulsed operation, and more than two points for quasiperiodic or irregular dynamics. For the chosen feedback parameters, we find that the system operates cw when $\tau_1 = \tau_2$ regardless the reinjection strength. When τ_2 increases, the cw solution becomes unstable and a limit cycle with small amplitude appears. This stage is followed by a rapid increase of the limit cycle amplitude; hence, pulses with large extinction ratio are obtained over a wide interval of τ_2. This interval defines a resonance width and an optimum reinjection time for which the highest output power and the shortest pulse width are obtained. Further increasing τ_2 yields windows of irregular pulsations. The overall structure consists of tongues of mode locking that qualitatively repeat every $\tau_2 \approx n\tau_1$, with n an integer number. While the tongues bifurcate supercritically for weak feedback, we have found that they become subcritical and can present bistability for stronger feedback. Figure 4(b) demonstrates that the ML period increases over the tongues by a 0.4% the fundamental period, the fact that allows for small timing adjustments with τ_2.

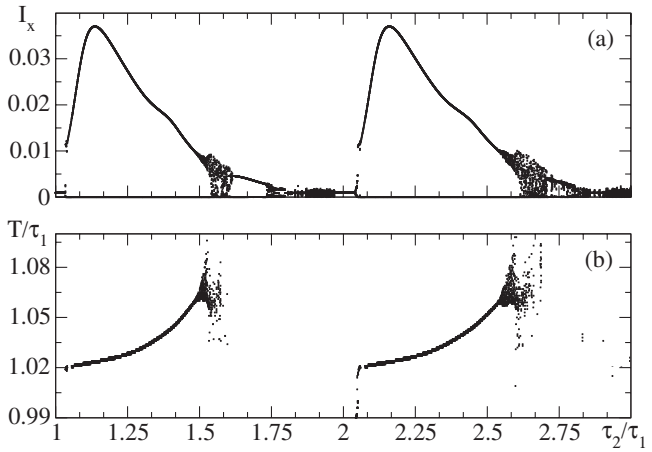

FIG. 4. (a) Bifurcation diagram for the x_{LP} component as a function of τ_2. (b) Mode-locking period. Parameters: $\eta = 0.025$, $\beta = 0.1$, and $P = -0.01$.

In order to provide a more detailed description of the pulse formation, we have analyzed the stability of the monochromatic solutions of the system (1)–(3). They provide the backbone upon which the ML solution is nascent as a secondary Hopf bifurcation. The monochromatic solutions can readily be expressed as $\vec{E} = (E_x, E_y)$. Two types of solutions exist: a family of external-cavity modes (ECMs) $\vec{E} = E_0(\cos\theta, e^{i\phi}\sin\theta)$ and a single y_{LP} mode $\vec{E} = (0, \sqrt{P})$ which is only active above the solitary VCSEL threshold. In these expressions, $E_0 = \rho\exp(i\omega t)$ are the well-known ECMs of a laser with optical feedback [15], and $\theta = \arctan(\beta/\eta)$, $\phi = \omega\Delta\tau + \Omega$, and $\Delta\tau = \tau_2 - \tau_1$ control the polarization state of the ECMs. Although the structure of ECMs is similar to that of laser with optical feedback, the stability of ECMs and quasiperiodic states is drastically modified by the reinjection, which qualitatively explains the occurrence of stable mode locking.

The study of the monochromatic solutions is complemented with a nonlinear analysis of the dynamical system using the continuation package DDEbifTool [16]. We have followed the secondary Hopf bifurcations arising on the ECMs. In the absence of reinjection, quasiperiodic solutions do not evolve into highly anharmonic patterns and they predominantly form bridges connecting different ECMs [17,18]. This scenario is drastically changed in the presence of reinjection. Figure 5 shows a typical bifurcation scenario. The first instability is a secondary Hopf bifurcation at $\eta_H \approx 0.0123$. The quasiperiodic modulation nascent from such an ECM evolves sharply into an anharmonic modulation when the feedback rate η is increased, and the oscillation frequency is always close to $1/\tau_1 \sim 1$ GHz as imposed by the round-trip frequency. In this example, the branch of the solution does not terminate on the right end on an ECM for higher values of the feedback rate η. However, we have found more intricate situations where a first branch of ML was found to make bridges connecting the same ECM, while for higher feedback rates a main ML branch arises.

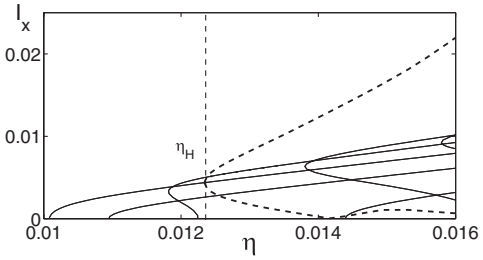

FIG. 5. ECMs intensity as function of η. A secondary Hopf bifurcation appears for $\eta_H \approx 0.0123$ evolving into a ML state with η. Parameters: $\beta = 0.12$, $\tau_2 = 1.5\tau_1$, $P = -0.01$.

The Hopf bifurcation arises from the interplay of three different time scales, namely, the external-cavity round-trip time τ_1, the reinjection delay τ_2, and the gain recovery time T_G. Any fluctuation in the power of the lasing polarization will interact with the active medium at two later stages. Thus, when a pulse is emitted, two delayed replicas arrive onto the active medium after times τ_1 and τ_2, respectively. The arrival of the first replica induces a depletion in population inversion, which can be further enhanced if the second replica arrives when the population reaches the minimum value. The subsequent recovery of the population will open a window of net gain after a time T_G and trigger the emission of a pulse. This might lead to stable ML operation at the fundamental repetition rate only if the time T_G roughly coincides with τ_1, while it would lead to harmonic ML if it coincides with a submultiple of τ_1. If these conditions are not met the background self-starts and ML becomes incomplete. The system self-adjusts to find a condition for matching these three different time scales. Timing adjustments are possible since the time T_G is quite sensitive to the pulse energy and to the arrival of the reinjection pulse.

The above explanation can be linked with the classical arguments given for passive mode locking with saturable absorbers. On one hand, the preference for pulsing against cw emission can be understood in terms of a minimum gain principle; i.e., the preferred solution is that requiring less gain to operate. Saturable absorbers induce passive mode locking since pulses can more easily bleach the absorption than cw. In our scheme the VCSEL plays the role of a laser amplifier. The amplification of two orthogonally polarized signals is subject to XPGM, which implies a gain penalty for amplifying both signals simultaneously. This gain penalty is different whether two cw signals or two time-shifted pulses are amplified. For appropriate reinjection conditions, the gain penalty for cw amplification is larger than for two time-shifted pulses, thus it discriminates the cw solution. On the other hand, the reinjection provides a way to control the recovery time of the gain T_G. The process is self-adjusted with the pulse energy in order to open a narrow window of net gain around the pulses.

In summary, we have demonstrated that a vertical-external-cavity surface-emitting laser can be passively mode locked without using any saturable absorber nor an external oscillator. Mode locking is accomplished by forcing the lasing polarization of the laser to interact with its replica after being delayed and rotated to the orthogonal polarization orientation. The system has been described in the framework of a generic rate equation model. We have applied direct numerical integration and continuation methods in order to characterize the solutions and identify the underlying mechanisms leading to mode locking. We have demonstrated that the reinjection enhances the population pulsations as a result of a Hopf bifurcation which develops into stable mode locking.

In the present example, the available optical bandwidth is limited to few tens of GHz. Nonetheless, the results are in the state of the art of electrically driven VECSELs mode locked with saturable absorber mirrors [9]. We have found stable mode-locked pulses of few tens of picoseconds at multi-GHz repetition rates. The pulse width can be further shortened by increasing the optical bandwidth upon replacement of the VCSEL by a vertical-cavity optical amplifier (VCSOA) subject to strong optical feedback. Alternatively, the proposed mechanism can be also applied to edge-emitting lasers, where TE is reinjected into TM polarization modes. Future perspectives include the realization of mode-locked prototypes and the refinement of the theoretical description.

This work has been founded through the Project No. TEC2006-13887-C05-03/TCM. J. J. acknowledges support from the program Juan de la Cierva of the MEC. J. M. acknowledges support from the Program No. I3P-PC2003 and the Project CONOCE-2: No. FIS2004-00953.

[1] A. Gordon and B. Fischer, Phys. Rev. Lett. **89**, 103901 (2002).
[2] H. A. Haus, IEEE J. Sel. Top. Quantum Electron. **6**, 1173 (2000).
[3] Y. J. Wen, H. F. Liu, and D. Novak, IEEE J. Quantum Electron. **37**, 1183 (2001).
[4] E. P. Ippen, Appl. Phys. B **58**, 159 (1994).
[5] X. Yang, Z. Li, E. Tangdiongga, D. Lenstra, G. D. Khoe, and H. J. S. Dorren, Opt. Express **12**, 2448 (2004).
[6] F. Marino, L. Furfaro, and S. Balle, Appl. Phys. Lett. **86**, 151116 (2005).
[7] N. Laurand, S. Calvez, M. Dawson, and E. Kelly, Appl. Phys. Lett. **87**, 231115 (2005).
[8] T. Heil, I. Fischer, W. Elsaesser, J. Mulet, and C. R. Mirasso, Phys. Rev. Lett. **86**, 795 (2001).
[9] A. C. Tropper, H. D. Foreman, A. Garnache, K. G. Wilcox, and S. H. Hoogland, J. Phys. D: Appl. Phys. **37**, R75 (2004).
[10] M. San Miguel, Q. Feng, and J. V. Moloney, Phys. Rev. A **52**, 1728 (1995).
[11] T. Heil, A. Uchida, P. Davis, and T. Aida, Phys. Rev. A **68**, 033811 (2003).
[12] See, e.g., T. Heil, I. Fischer, W. Elsasser, B. Krauskopf, K. Green, and A. Gavrielides, Phys. Rev. E **67**, 066214 (2003) and references therein.
[13] A. Tabaka, M. Peil, M. Sciamanna, I. Fischer, W. Elsasser, H. Thienpont, I. Veretennicoff, and K. Panajotov, Phys. Rev. A **73**, 013810 (2006).
[14] K. Jasim, Q. Zhang, A. V. Nurmikko, E. Ippen, A. Mooradian, G. Carey, and W. Ha, Electron. Lett. **40**, 34 (2004).
[15] R. Lang and K. Kobayashi, IEEE J. Quantum Electron. **16**, 347 (1980).
[16] K. Engelborghs, T. Luzyanina, and G. Samaey, K. U. Leuven Technical Report No. TW-330, 2001.
[17] D. Pieroux, T. Erneux, B. Haegeman, K. Engelborghs, and D. Roose, Phys. Rev. Lett. **87**, 193901 (2001).
[18] M. Sciamanna, T. Erneux, F. Rogister, O. Deparis, P. Mégret, and M. Blondel, Phys. Rev. A **65**, 041801(R) (2002).